Tuning Synthetic Semiflexible Networks by Bending Stiffness

Carsten Schuldt,[1,2] Jörg Schnauß,[1,2] Tina Händler,[1,2] Martin Glaser,[1,2] Jessica Lorenz,[2] Tom Golde,[1]
Josef A. Käs,[1] and David M. Smith[2*]

[1]*Institute of Experimental Physics I, Universität Leipzig, Linnéstraße 5, 04103 Leipzig, Germany*
[2]*Fraunhofer Institute for Cell Therapy and Immunology, Perlickstraße 1, 04103 Leipzig, Germany*

The mechanics of complex soft matter often cannot be understood in the classical physical frame of flexible polymers or rigid rods. The underlying constituents are semiflexible polymers, whose finite bending stiffness (κ) leads to nontrivial mechanical responses. A natural model for such polymers is the protein actin. Experimental studies of actin networks, however, are limited since the persistence length ($l_p \propto \kappa$) cannot be tuned. Here, we experimentally characterize this parameter for the first time in entangled networks formed by synthetically produced, structurally tunable DNA nanotubes. This material enabled the validation of characteristics inherent to semiflexible polymers and networks thereof, i.e., persistence length, inextensibility, reptation, and mesh size scaling. While the scaling of the elastic plateau modulus with concentration $G_0 \propto c^{7/5}$ is consistent with previous measurements and established theories, the emerging persistence length scaling $G_0 \propto l_p$ opposes predominant theoretical predictions.

Semiflexible polymers are of fundamental importance to biological systems due to their ability to form stable scaffolds at low volume fractions, with their voids providing free space for the molecular transport and metabolic processes necessary for active, living matter [1,2].

This special class of polymers is distinguished by their nonvanishing bending rigidity, featuring an outstretched configuration while still subjected to strong thermal fluctuations [1]. Within the wormlike chain model [3,4], this stiffness is described by the persistence length (l_p), which represents the decay constant of the tangent-tangent correlation [5]. When the contour length (l_c) is comparable to l_p, polymers are considered semiflexible [1]. Networks of these filamentous constituents in the entangled concentration regime (mesh size $\xi \leq l_p$) have been subject to considerable studies [6–10], but their central quantity l_p is still unexplored since it remained experimentally inaccessible to systematic variation for any given material. Sophisticated theoretical approaches were built starting from the single-filament level in order to describe the emergence of the nontrivial mechanical behaviors since classical models for flexible chains or rigid rods are not directly applicable [2]. Depending on the microscopic models for network architecture and load transduction to the individual filament, markedly different scaling predictions for the linear elastic plateau shear modulus (G_0) with respect to concentration (c) and l_p have been suggested [7,11–13].

The concentration scaling is readily experimentally accessible, and corresponding theoretical predictions have been rigorously verified [12,14–16]. In pioneering experimental work, the cellular biopolymer actin was established as a model system for semiflexible filaments and is still considered the gold standard [6,12,13,15,17–20], although some of its material-specific effects such as the unidirectional "treadmilling" of monomers from one end toward the other cannot be considered a general characteristic of semiflexible polymers [1]. However, the scaling of network elasticity with respect to l_p still remained experimentally inaccessible for this model system since the l_p of actin cannot be varied as an independent parameter [14]. This limitation is inherent for all biopolymers and thus a comprehensive validation of the published theoretical predictions is still pending to date.

To resolve this important dependency and to overcome the natural limitation imposed by the fixed l_p of actin, we employed synthetically produced, tile-based DNA tubes [21], which were previously demonstrated to have tunable mechanical properties, i.e., stiffness [22]. They are soluble in water and stable for months in adequate pH and ionic conditions without displaying aging effects typical of protein-based filaments [21]. To assemble these tubes, we used a set of n ($4 \leq n \leq 14$) distinct, partially complementary DNA oligonucleotides (each 42 bases in length, see Supplemental Material [23], Sec. I), which hybridize to a half overlapping ring of n interconnected DNA helices [Figs. 1(a) and 1(b)] [21]. Axial sticky ends trigger a selective addition of matching oligonucleotides, inducing an effective polymerization of tubes with a contour length distribution comparable to actin [21]. Depending on the set of n strands chosen, n-helix tubes (nHTs) with a uniform circumference were formed. It was previously shown that the l_p of these nHTs scales with their second moment of inertia (see Ref. [22]). Thus, these DNA n-helix tubes are purely synthetic polymers, programmable in their circumference and accordingly in their l_p [Fig. 1(b)].
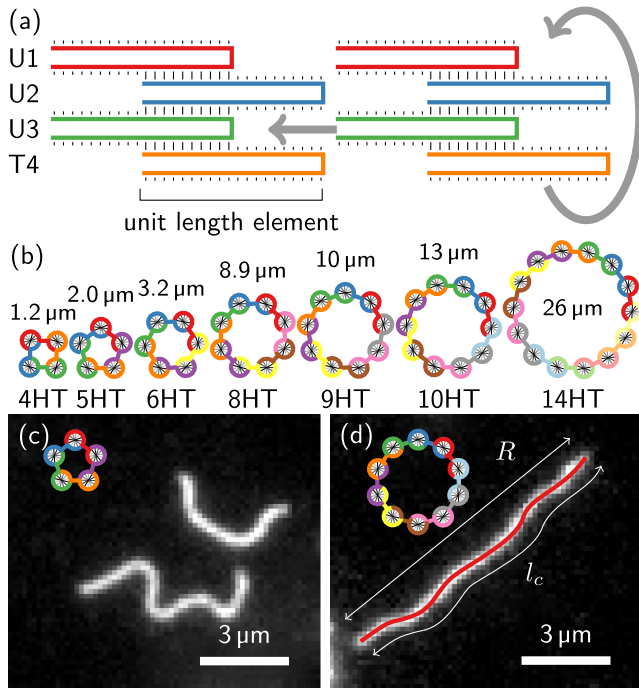
FIG. 1. n-helix tube (nHT) filament architecture. (a) Schematic of the assembly of a 4HT formed of four distinct 42-mers. Adjacent single-stranded DNA oligonucleotides share continuous complementary sections of 10 and 11 bases in length (long black ticks). Boundary strands U1 and T4 feature complementary sequences as well, enabling the formation of a tubelike ring from the planar sheet structure. The half-staggered motif of these rings with sticky ends on both sides promotes polymerizationlike axial growth. (b) Cross sections of all seven different nHTs employed in this study with according measured values for l_p. Strand numbers range from 4 to 14HT and l_p from 1.2 to 26 μm, respectively. (c),(d) Epifluorescent image of Cy3-labeled adsorbed nHTs. Left: 5HT. Right: 10HT. The red overlay is the filament contour approximated by image analysis with end-to-end distance R and contour length l_c [33]. (a)and (b) Inspired by Yin *et al.* [21].

We confirmed and extended upon previous measurements of l_p that were based on freely fluctuating nHTs [22] by evaluating epi-fluorescence images of more than 100 adsorbed, single filaments [Figs. 1(c) and 1(d)] for each of the seven different nHTs used here. One of the constituent oligonucleotides was substituted by a Cy3 conjugated analog for fluorescent imaging. Image-based tracking and fitting of the tangent-tangent correlation yielded a range of l_p from (1.2 ± 0.1) μm (4HT) to (26 ± 5) μm (14HT). Applying a kurtosis analysis (see Supplemental Material [23], Sec. II), we could exclude any possible effects from surface interactions during adsorption and found the same values and quantitative trend for l_p as reported for freely fluctuating tubes [22].

While the determination of l_p was performed in dilute samples to measure this intrinsic property, reptation experiments were performed in the same concentration regime as

used for the rheology experiments. A small number of fluorescently labeled tubes were embedded in an unlabeled network and their snakelike reptation motion was recorded and tracked as described for the l_p determination (for more details see Supplemental Material [23], Sec. III).

Using this synthetic system, we were able to quantify the changes in emergent network mechanics resulting from systematically varying l_p over more than 1 order of magnitude, without making any changes to the underlying material. Each type of nHT forms isotropic networks [Figs. 2(a) and 2(b)], which allowed us to investigate the mechanical response of these networks with dynamic shear rheology. After an equilibration of 2 h, a series of frequency (f) and strain (γ) sweeps was performed to characterize intrinsic mechanics as well as potential aging effects: (i) short f sweep ($\gamma = 5\%$, $f = 0.01$ to 30 Hz, 5 data points per decade), (ii) long f sweep ($\gamma = 5\%$, $f = 0.001$ to 30 Hz, 21 data points per decade), (iii) short f sweep, (iv) γ sweep ($f = 1$ Hz, $\gamma = 0.0125\%$ to 100%, 20 data points per decade), (v) short f sweep, and (vi) γ sweep. Different passivation techniques to inhibit air-liquid interface effects were also tested, yielding consistent results (cf. Supplemental Material [23], Sec. V).

Frequency sweeps revealed the predominately elastic response in the linear regime [Fig. 2(c)]. In the frequency range of 10^{-3} to 10 Hz, the elastic modulus G' exceeded the viscous modulus G'' by approximately 1 order of magnitude and no crossover between the two moduli was observed. G' was nearly constant in this range and showed a broad rubber plateau over four decades. This characteristic is in contrast to previous measurements on actin [20], where long-term relaxation and the associated viscoelastic crossover might be superimposed by treadmilling effects [1,13] resulting from unbalanced binding kinetics of monomeric actin at filament ends. In contrast, the nHTs employed here
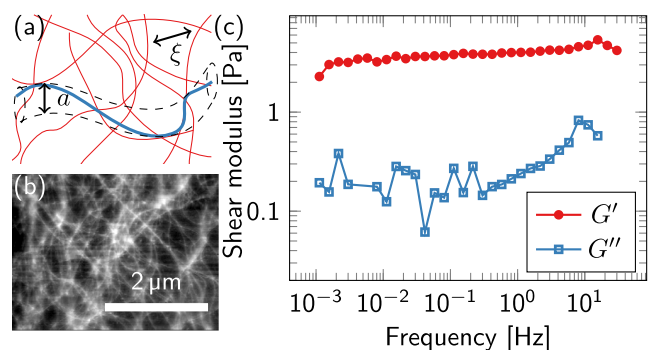

FIG. 2. Network elasticity. (a) Schematic of a semiflexible filament meshwork with mesh size ξ. A test polymer (blue) of contour length l_c is confined by the background of red filaments to a tube of width a. (b) AFM image of an 8HT network formed at 4 μM. (c) Frequency resolved viscoelastic properties of an 8HT network at 6 μM probed by bulk shear rheology at a strain of 5%. A pronounced elastic rubber plateau over more than 4 orders of magnitude is characteristic of all nHTs.

are not influenced by any type of treadmilling due to the high stability of hybridized DNA segments in the typical measurement conditions. The dominance of G', as well as the frequency independence of the rubber plateau, are universal features for all seven nHTs and all concentrations studied. We derived the scaling of the elastic plateau modulus with respect to concentration from frequency sweeps with $G_0 = G'(1 \text{ Hz}, 5\%)$. Between 0.5 and 20 μM, G_0 increased monotonically between 50 mPa and 20 Pa for all nHTs [Fig. 3(a)]. Given a power law $G_0 \propto c^\alpha$, exponents accumulated around $\alpha = 7/5$ [Fig. 3(b)]. 4HTs at low concentrations are very soft (low sub Pascal range) falling below the sensitivity of the rheometer.

These measurements allowed us to evaluate the scaling of G_0 with respect to l_p [Fig. 3(c)]. Circumferences of the nHTs were translated into l_p with values determined as described above. Each curve in Fig. 3(c) represents one specific concentration. With increasing l_p, we found a monotonic increase of G_0. Given a power law $G_0 \propto l_p^\beta$, exponents were found to accumulate around $\beta = 1$ [Fig. 3(d)]. These scaling results were independent of the choice of strain and strain rate (cf. Supplemental Material [23], Sec. VII). In conclusion, these shear rheology measurements accessed the concentration and l_p dependencies of G_0 and revealed an overall scaling relation of

$$G_0 \propto c^{7/5} l_p. \qquad (1)$$

To validate the applicability of our findings to the conceptual framework of an entropically fluctuating, entangled network, we ensured that these DNA nHT networks were indeed only topologically entangled and not physically cross-linked. In particular, we investigated if

these networks exhibited strain stiffening and whether single filaments displayed snakelike reptation within the background network. These measurements revealed no sign of strain stiffening [Fig. 4(a)], which is considered a general characteristic of cross-linked networks [8,34] (cf. Supplemental Material [23], Sec. IV). Additionally, filaments were observed to reptate freely in tubelike regions within the networks [Fig. 4(b) and Supplemental Material [23], Sec. III] [35]. This characteristic thermal motion for entangled networks would be suppressed by cross-links [36]. Furthermore, spatiotemporal traces of reptating filaments revealed the dependence of the network mesh size on the monomer concentration was comparable to $\xi \propto c^{-1/2}$ [Fig. 4(b), inset]. This behavior was consistent with our own reptation-based data on actin filaments, as well as both the predicted [35] and reported scalings for networks of semiflexible polymers as measured by microparticle diffusion [37]. Throughout all different elasticities, the mesh size was at the micrometer scale and shear elasticity dominated viscosity, which could be freely programmed by altering the nanoscale architecture of the underlying synthetic filaments. Because of the newly discovered linear l_p scaling of G_0, the bulk mechanics of this network could be precisely tuned over a broad range while keeping the mesh size constant, in contrast to the structural impact of simply increasing the material concentration. Finally, the inextensible nature of DNA nHTs was demonstrated through analysis of reptation data; filament fluctuations in equilibrium revealed bending modes without thermally excited stretching modes (see Supplemental Material [23], Sec. IV).

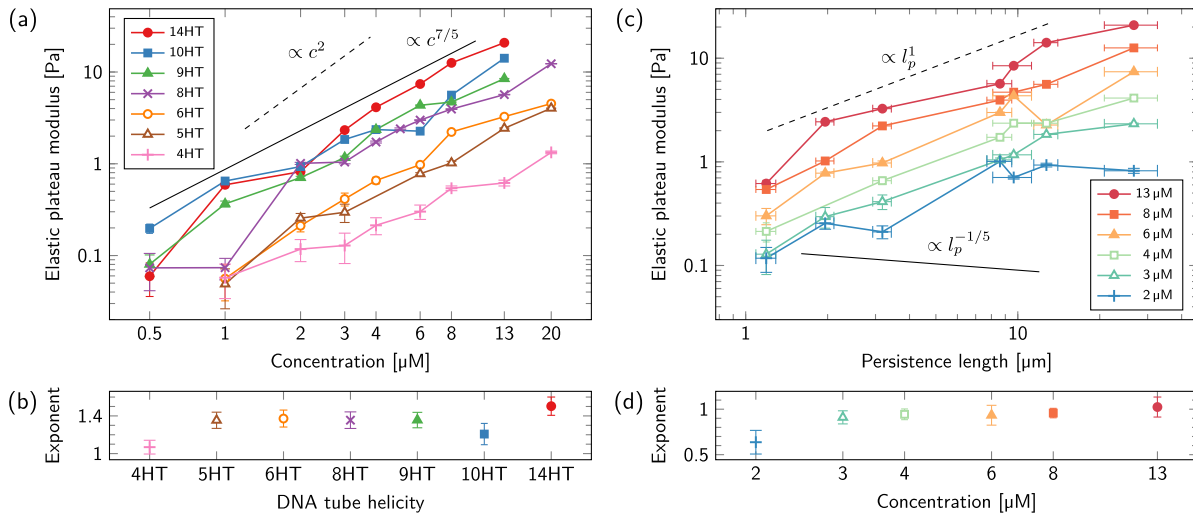Consequently, the DNA nHT networks can be considered purely entangled and compare well to the previously

FIG. 3. G_0 scaling of nHT networks. (a) The concentration scaling for networks of different nHT is plotted. Predicted power laws from the tube model and unit cell approach are given by black and dashed lines, respectively. (b) Least-squares approximations yielded the actual power law exponents for all nHT, which accumulated around $\alpha \approx 7/5$. (c) The persistence length scaling for networks of different concentration is shown. (d) Approximated power law exponents yielded a mean exponent of $\beta \approx 1$. In summary, we found the elastic shear modulus to scale as $G_0 \propto c^{7/5} l_p$.
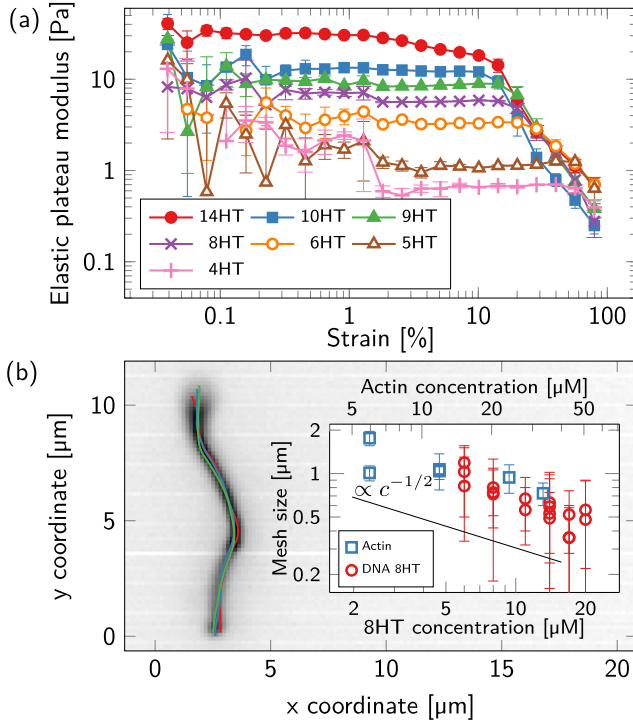
FIG. 4. Linearity and microscopic mesh size. (a) Strain sweeps of $G'(1\,\text{Hz})$ feature a broad linear elastic plateau for small strains. Beyond a characteristic strain G' breaks off irreversibly depending on nHT. (b) Microscopic reptation of a single labeled DNA 8HT embedded in a network of the same type of filaments. The summation fluorescent image of 600 sampled configurations is overlaid by three exemplary filaments as found by image analysis ($c = 14\ \mu$M). Inset: Mesh size of actin and DNA 8HT networks as derived from such reptation analysis at different concentrations. Monomeric concentrations are shifted by the chain length conversion factor $x = l_{\text{monomer},n\text{HT}}/l_{\text{monomer,actin}} \simeq 2.5$ to compare the same concentrations of contour length per unit volume. Mesh sizes are on the same order of magnitude and decrease with concentration. Theoretical scaling prediction $\xi \propto c^{-1/2}$ is indicated by the solid line [35].

employed model system of actin networks. The predominant theoretical description of entangled networks is the *tube model* [18,38]. Within this framework, the many-body problem of a network of filaments is reduced to a single fluctuating test filament, with all other polymers conceptualized as an effective tube constricting its motions [12,13,39]. Each collision with this tube contributes on the order of $k_B T$ to the free energy of the system, with the sum of all collisions constituting the shear modulus. Shear deformations are modeled as a compression of this tube yielding the scaling $G_0 \propto l_p^{-1/5} c^{7/5}$, as also shown in numerical simulations [16]. This trend has also emerged from different conceptual realizations of the interaction with the tube [39]. Notably, these models predict a peculiar decrease of overall network elasticity as the individual components become stiffer, i.e., with increasing l_p, due to the entropic origin of the mechanical response. However,

this important parameter was never comprehensively accessible to any previous experimental studies, and, therefore, never rigorously determined in an independent manner.

One attempt aimed to alter the "effective" persistence length of actin by varying solvent conditions [14]. A persistence length scaling consistent with an effective medium implementation of the tube model was reported [39], although only based on two independent l_p values. This clearly illustrates the natural limitations of biopolymers such as actin as comprehensive models systems for semiflexible filaments. Intermediate filaments such as vimentin with a significantly lower l_p also fall into this class and reveal typical semiflexible mechanical properties [40]. However, both biopolymers not only differ in their mechanical properties but also in their underlying molecular structure and equilibrium-state dynamics, thereby rendering the consistent derivation of l_p scaling laws difficult.

Here, we present the first in-depth study on both parameters of concentration and persistence length performed without changing the underlying material. Within our study, we corroborate the concentration scaling $G_0 \propto c^{7/5}$ as predicted by the tube model [39], which was already experimentally confirmed for actin networks [12,14] and more generally in numerical simulations [16]. Though confirming several key characteristics of the tube model, we clearly find that G_0 scales linearly with l_p—in strong disagreement with the tube model's prediction $G_0 \propto l_p^{-1/5}$. The overall scaling of the elastic modulus shown here of $G_0 \propto c^{7/5} l_p$ cannot be explained with any existing theory. The simplistic unit cell approach, for instance, predicts the linear l_p scaling correctly, but overestimates the impact of concentration [11,41]. Another bending dominated theoretical approach is the so-called affine network model, which assumes local deformations, namely, affine contraction and stretching of individual filaments. This approach yields an elastic plateau modulus which increases with persistence length $c^{11/5} l_p^{7/5}$ [7], although it has been shown experimentally that this model most likely applies to cross-linked systems [8,42] and is inappropriate to describe the results of our nHT study.

Bending dominated theories, in particular the oversimplifying athermal unit cell model mentioned above [11,41], predict the significantly stronger trend of l_p scaling more closely than the tube model. We therefore speculate that the tube model demands adjustment with respect to further internal energy contributions from filament bending, whose additional contributions scale linearly with filament stiffness [41].

These findings contradict the established picture of semiflexible polymer networks, which are distinguished by the central quantity l_p. Key aspects of the established tube model, such as reptation, inextensibility, and the correct concentration scaling were indeed proven for this *de novo* model system of DNA nHTs. In contrast, through rigorously studying the impact of l_p for the first time, we found striking disagreement with the prediction of the tube model. This observation is impossible with other known

model systems, since they lacked the ability to tune l_p freely [12] or deterministically [43], were cross-linked [42], were subjected to treadmilling [1,13], or the ratio l_c/l_p did not fit within the semiflexible regime [43]. Because of the structurally modular, self-assembling nature of the DNA nHTs, other parameters of semiflexible networks such as the addition of physical cross-links might be readily accessible in an equally programmable way. Since all of these material properties are decoupled for the first time, this unique model system will stimulate further development of our understanding of the emerging mechanics of semiflexible polymer networks.

---

*david.smith@izi.fraunhofer.de

[1] F. Huber, J. Schnauß, S. Rönicke, P. Rauch, K. Müller, C. Fütterer, and J. Käs, Emergent complexity of the cytoskeleton: from single filaments to tissue, Adv. Phys. **62**, 1 (2013).

[2] C. Broedersz and F. MacKintosh, Modeling semiflexible polymer networks, Rev. Mod. Phys. **86**, 995 (2014).

[3] O. Kratky and G. Porod, Röntgenuntersuchung gelöster Fadenmoleküle, Recl. Trav. Chim. **68**, 1106 (1949).

[4] N. Saitô, K. Takahashi, and Y. Yunoki, The statistical mechanical theory of stiff chains, J. Phys. Soc. Jpn. **22**, 219 (1967).

[5] M. Doi and S. F. Edwards, The theory of polymer dynamics, *The Theory of Polymer Dynamics*, 1st ed., International Series of Monographs on Physics (Oxford University Press, Oxford, 1986), Vol. 73.

[6] O. Mueller, H. E. Gaub, M. Baermann, and E. Sackmann, Viscoelastic moduli of sterically and chemically cross-linked actin networks in the dilute to semidilute regime: measurements by oscillating disk rheometer, Macromolecules **24**, 3111 (1991).

[7] F. C. MacKintosh, J. Käs, and P. A. Janmey, Elasticity of Semiflexible Biopolymer Networks, Phys. Rev. Lett. **75**, 4425 (1995).

[8] M. L. Gardel, J. H. Shin, F. C. MacKintosh, L. Mahadevan, P. Matsudaira, and D. A. Weitz, Elastic behavior of cross-linked and bundled actin networks, Science **304**, 1301 (2004).

[9] D. A. Fletcher and R. D. Mullins, Cell mechanics and the cytoskeleton, Nature (London) **463**, 485 (2010).

[10] A. Sonn-Segev, A. Bernheim-Groswasser, H. Diamant, and Y. Roichman, Viscoelastic Response of a Complex Fluid at Intermediate Distances, Phys. Rev. Lett. **112**, 088301 (2014).

[11] K. Kroy and E. Frey, Force-Extension Relation and Plateau Modulus for Wormlike Chains, Phys. Rev. Lett. **77**, 306 (1996).

[12] B. Hinner, M. Tempel, E. Sackmann, K. Kroy, and E. Frey, Entanglement, Elasticity, and Viscous Relaxation of Actin Solutions, Phys. Rev. Lett. **81**, 2614 (1998).

[13] H. Isambert and A. C. Maggs, Dynamics and rheology of actin solutions, Macromolecules **29**, 1036 (1996).

[14] M. Tassieri, R. M. L. Evans, L. Barbu-Tudoran, G. Khaname, J. Trinick, and T. Waigh, Dynamics of Semiflexible Polymer Solutions in the Highly Entangled Regime, Phys. Rev. Lett. **101**, 198301 (2008).

[15] J. Liu, M. L. Gardel, K. Kroy, E. Frey, B. D. Hoffman, J. C. Crocker, A. R. Bausch, and D. A. Weitz, Microrheology Probes Length Scale Dependent Rheology, Phys. Rev. Lett. **96**, 118104 (2006).

[16] H. Hinsch and E. Frey, Non-Affine Shear Modulus in Entangled Networks of Semiflexible Polymers, arXiv:0907.1875.

[17] J. Käs, H. Strey, J. Tang, D. Finger, R. Ezzell, E. Sackmann, and P. Janmey, F-actin, a model polymer for semiflexible chains in dilute, semidilute, and liquid crystalline solutions, Biophys. J. **70**, 609 (1996).

[18] D. C. Morse, Viscoelasticity of Concentrated Isotropic Solutions of Semiflexible Polymers. 2. Linear Response, Macromolecules **31**, 7044 (1998).

[19] A. Palmer, T. G. Mason, J. Xu, S. C. Kuo, and D. Wirtz, Diffusing wave spectroscopy microrheology of actin filament networks, Biophys. J. **76**, 1063 (1999).

[20] M. L. Gardel, M. T. Valentine, J. C. Crocker, A. R. Bausch, and D. A. Weitz, Microrheology of Entangled F-Actin Solutions, Phys. Rev. Lett. **91**, 158302 (2003).

[21] P. Yin, R. F. Hariadi, S. Sahu, H. M. T. Choi, S. H. Park, T. H. LaBean, and J. H. Reif, Programming DNA tube circumferences, Science **321**, 824 (2008).

[22] D. Schiffels, T. Liedl, and D. K. Fygenson, Nanoscale structure and microscale stiffness of DNA nanotubes, ACS Nano **7**, 6700 (2013).

[23] See Supplemental Material at http://link.aps.org/supplemental/10.1103/PhysRevLett.117.197801 for comprehensive Materials and Methods section and auxiliary data, which includes Refs. [24–32].

[24] B. Gentry, D. Smith, and J. Käs, Buckling-induced zebra stripe patterns in nematic F-actin, Phys. Rev. E **79**, 031916 (2009).

[25] C. Rivetti, M. Guthold, and C. Bustamante, Scanning force microscopy of DNA deposited onto mica: equilibration versus kinetic trapping studied by statistical polymer chain analysis, J. Mol. Biol. **264**, 919 (1996).

[26] N. Mücke, L. Kreplak, R. Kirmse, T. Wedig, H. Herrmann, U. Aebi, and J. Langowski, Assessing the flexibility of intermediate filaments by atomic force microscopy, J. Mol. Biol. **335**, 1241 (2004).

[27] A. N. Semenov, Dynamics of concentrated solutions of rigid-chain polymers. Part 1.—Brownian motion of persistent macromolecules in isotropic solution, J. Chem. Soc., Faraday Trans. 2, **82**, 317 (1986).

[28] H. Hinsch, J. Wilhelm, and E. Frey, Quantitative tube model for semiflexible polymer solutions, Eur. Phys. J. E **24**, 35 (2007).

[29] U. Aebi, R. Millonig, H. Salvo, and A. Engel, The three-dimensional structure of the actin filament revisited, Ann. N.Y. Acad. Sci. **483**, 100 (1986).

[30] S. Yamada, D. Wirtz, and P. A. Coulombe, The mechanical properties of simple epithelial keratins 8 and 18: discriminating between interfacial and bulk elasticities, J. Struct. Biol. **143**, 45 (2003).

[31] C. Liu, J. He, E. v. Ruymbeke, R. Keunings, and C. Bailly, Evaluation of different methods for the determination of the plateau modulus and the entanglement molecular weight, Polymer **47**, 4461 (2006).

[32] F. G. Schmidt, B. Hinner, and E. Sackmann, Microrheometry underestimates the values of the viscoelastic moduli in measurements on F-actin solutions compared to macrorheometry, Phys. Rev. E **61**, 5646 (2000).

[33] M. B. Smith, H. Li, T. Shen, X. Huang, E. Yusuf, and D. Vavylonis, Segmentation and tracking of cytoskeletal filaments using open active contours, Cytoskeleton (Hoboken, N.J.) **67**, 693 (2010).

[34] C. Storm, J. J. Pastore, F. C. MacKintosh, T. C. Lubensky, and P. A. Janmey, Nonlinear elasticity in biological gels, Nature (London) **435**, 191 (2005).

[35] P. de Gennes, P. Pincus, R. Velasco, and F. Brochard, Remarks on polyelectrolyte conformation, J. Phys. (Paris) **37**, 1461 (1976).

[36] J. Käs, H. Strey, and E. Sackmann, Direct imaging of reptation for semiflexible actin filaments, Nature (London) **368**, 226 (1994).

[37] C. F. Schmidt, M. Baermann, G. Isenberg, and E. Sackmann, Chain dynamics, mesh size, and diffusive transport in networks of polymerized actin: a quasielastic light scattering and microfluorescence study, Macromolecules **22**, 3638 (1989).

[38] P.-G. de Gennes, Scaling concepts in polymer physics, *Scaling Concepts in Polymer Physics*, 7th ed. (Cornell University Press, London, 1979).

[39] D. Morse, Tube diameter in tightly entangled solutions of semiflexible polymers, Phys. Rev. E **63**, 031502 (2001).

[40] B. Nöding and S. Köster, Intermediate Filaments in Small Configuration Spaces, Phys. Rev. Lett. **108**, 088101 (2012).

[41] R. L. Satcher, Jr. and C. F. Dewey, Jr., Theoretical estimates of mechanical properties of the endothelial cell cytoskeleton, Biophys. J. **71**, 109 (1996).

[42] M. Jaspers, M. Dennison, M. F. J. Mabesoone, F. C. MacKintosh, A. E. Rowan, and P. H. J. Kouwer, Ultra-responsive soft matter from strain-stiffening hydrogels, Nat. Commun. **5**, 5808 (2014).

[43] N. Fakhri, D. A. Tsyboulski, L. Cognet, R. B. Weisman, and M. Pasquali, Diameter-dependent bending dynamics of single-walled carbon nanotubes in liquids, Proc. Natl. Acad. Sci. U.S.A. **106**, 14219 (2009).